

***Comparative mineralogy of the ~2.7 Ga Soudan Iron Formation, Minnesota and the Deloro Iron Formation, Timmins, ON, and the Temagami Iron Formation, Temagami, ON.***

*Danielle Stolze*

*Department of Earth and Environmental Sciences, University of Minnesota Duluth*

*Advisor: Dr. Latisha Brengman*

**Project summary:** The purpose of this project was to compare the mineralogy of similarly aged rocks from the Soudan Iron Formation in Minnesota and the Temagami and Deloro Iron Formations in Ontario, Canada. After sample collection, we used thin section imaging and X-ray diffraction to analyse and compare the mineralogy of rock samples from each location. We found that the iron-bearing samples generally fell into two categories: those with a banded texture (for example TEMj-1 and TEM-CF) and those that appear to consist mostly of chert with iron phases interspersed randomly throughout the sample (for example AB-11-32). These mineralogical variations and textural relationships can help us infer more information about the depositional environments in each sample location.

**Goal:** The goal of this project was to compare mineral inventories of the Soudan Iron Formation near Soudan, Minnesota with rocks of a similar age near Timmins, Ontario and Temagami, Ontario. A comparison of the mineralogy and texture of these rocks could provide significant new insight into the evolution of environmental conditions during the Precambrian.

## Introduction

Banded Iron Formations (BIF) are silica- and iron-rich chemical sedimentary deposits that formed from >3.7 - 1.7 billion years ago during the Precambrian eon. The BIFs of northern Minnesota formed roughly 2.7 billion years ago in a subaqueous (underwater) volcanic environment when hot fluid circulated through existing rocks. The hydrothermal fluid leached out cations such as  $\text{Fe}^{2+}$  and silica ( $\text{H}_4\text{SiO}_4$ ), which then went into solution. Oxygen, which was produced by early photosynthesis, was also present in the water column and reacted with the iron to produce the cation  $\text{Fe}^{3+}$ , which then precipitated out. These iron-rich deposits alternated with silica-rich layers that precipitated when the hydrothermal fluid came into contact with cooler water farther from its source. This alternation of iron- and silica rich deposits produced the banding pattern we see in banded iron formations such as those of the Soudan Iron Formation.

## Geologic Context and Sample Descriptions

The samples analyzed in this project came from three locations: the Vermillion region of northeastern Minnesota and the Temagami and Timmins regions of Ontario, Canada. The iron formations at each location are comparable in age and on the surface seem similar in other ways as well. However, we wanted to do a more complete comparison of the mineralogical inventories of each rock unit. To do this, we analyzed samples collected from each locality using X-ray diffraction (XRD) and thin section imaging. XRD allowed us to precisely document the mineral contents of each sample, and the thin sections helped us identify textural relationships within each rock. This mineralogical data can help us learn more about the environmental conditions at the time these rocks were deposited.

The samples studied in this project generally fell into two categories: rocks composed predominantly of iron-bearing minerals and silica, and those that were apparently volcanic in origin and had experienced some form of low-grade metamorphism. To determine the exact mineral composition of each sample, XRD analysis was used. In the metamorphosed volcanics, I determined the presence of minerals such as chlorite, epidote, calcite, prehnite, and clay minerals. The presence of these phases indicates low grade metamorphism. Minerals like chlorite and epidote are often the product of aqueous alteration. The clay minerals are likely the result of a protolith rich in feldspars going through the process of hydrolysis, and they add to the evidence for alteration by water.

The iron-bearing samples can be divided into two groups: those that display alternating layers of iron and silica, and those that appear to consist mostly of chert. Minerals identified in XRD analysis of these samples include magnetite, hematite, and possibly Minnesotaitite, all of which are iron-bearing phases.

While the iron-bearing rocks of the Vermillion, Abitibi, and Temagami formations are similar in composition, their textures are quite varied. Some samples, such as TEM\_CF from the Temagami region, show straightforward bands of alternating iron and quartz compositions. Others, such as V-19-02, do not display layers at all. Instead, the iron phases are randomly interspersed throughout the very fine-grained quartz that makes up much of the sample. The iron phases in V-19-02 also have a "dingy" appearance that distinguishes them from the iron

phases of a sample like TEM\_CF, where the iron phases appear more polished. This dingy appearance could possibly indicate the presence of the iron-bearing mineral Minnesotaite.

### **Methods**

The two primary methods of analysis for this project were thin section imaging and X-ray diffraction. Thin sections are slices of rock that are polished down to a thickness of 30  $\mu\text{m}$  and placed on a glass slide. This allows us to see a sample's textural and mineralogical features in very fine detail. Thin sections for this project were made from samples collected from the field near Soudan, Minnesota, as well as from the Abitibi and Temagami regions of Ontario. A Nikon DS-Ri2-color camera was used to take images of the thin sections using a sNikon SMZ1270 stereoscope. Individual images were then stitched together in the application Adobe Photoshop to make a composite image.

X-ray diffraction (XRD) is a process used to determine the specific mineralogical content of a sample. XRD is based on Bragg's Law (  $n\lambda = 2d \sin \theta$  ) and identifies mineral phases by interpreting the constructive interference patterns generated by shooting X-rays at a sample. Peaks are generated when the planes of the mineral structure correspond to the angle of the X-ray. To prepare samples for XRD, each sample was cut into  $\sim 1$  cm cubes using a saw. All weathering rinds were removed. A Shallerbox SPEX 8350 was then used to break the cubes down into a fine, clay-sized powder with a homogeneous distribution of particles. The powder was stored in vials. For the actual XRD process, a 1 inch width by 2 inch height slide containing a homogenous sample of the powder was prepared. The slide was placed in the instrument. The duration of the analysis was approximately 45 minutes. After the XRD process was complete, mineral phases were identified using peak matching software (MDI JADE).

### **Results**

Table 1. This table summarizes the results of mineralogical analysis for the samples used in this project. A list of minerals identified using XRD is given, as well as a brief description of any textural relationships visible in thin sections. Two samples from each field work location are described in the table. In some cases, XRD analysis was not completed due to the Covid-19 pandemic, (TEMj-1, 1a), and therefore mineral composition has not been confirmed by XRD. Original XRD peak matching data can be found in the appendix.

Sample number	Mineral composition	Textural features	Location
V-19-02	Magnetite, quartz, possibly <b>Minnesotaite</b>	Nodular, fine grained quartz	Vermillion
V-19-07	Quartz, plagioclase (albite), muscovite, calcite, chlorite	Large quartz grains interspersed throughout matrix of clay minerals. Altered feldspar grains visible in the matrix.	Vermillion
AB-11-41	Quartz, possibly <b>Minnesotaite</b> , plagioclase (albite), graphite, chlorite, prehnite, calcite, kaolinite	Quartz nodules encased by rims of fine grained quartz. Altered feldspars and clay minerals are also present. Lapilli visible.	Abitibi
AB-11-32	Quartz, magnetite, possibly <b>Minnesotaite</b>	Very fine grained quartz with bands of slightly coarser quartz scattered throughout.	Abitibi
TEM-CF	Quartz, magnetite/hematite	Banding of alternating quartz and iron oxide bands.	Temagami
TEM-J1, 1a	Quartz, magnetite/hematite (no XRD data)	Alternating layers of quartz and iron oxides, thin bands of quartz present in places	Temagami

*Table 1. Table summarizing the mineral composition and textural relationships of several samples analyzed using XRD.*

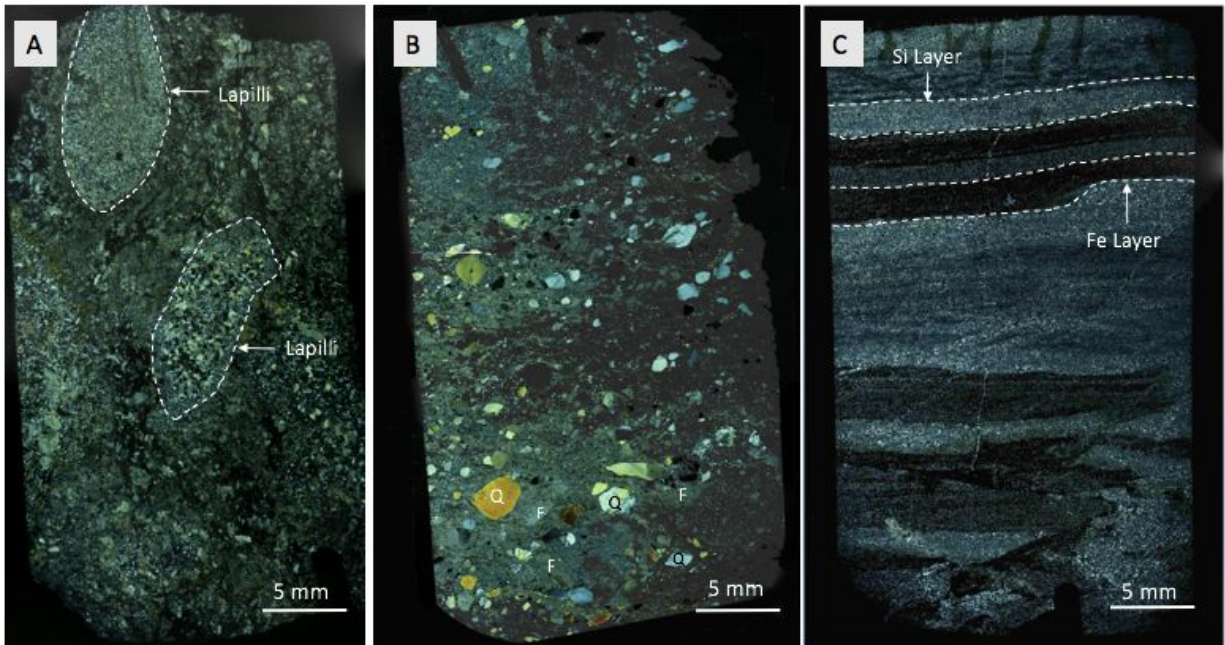


Figure 1. A side-by-side comparison of thin sections from samples AB-11-41 (A), V-19-07 (B), and TEMj-1 (C).

Figure 1 is a side-by-side comparison of samples AB-11-41, V-19-07, and TEMj-1 that we used to compare textural relationships and mineral composition in thin section. These specific samples were chosen because they represent the three main types of rocks that we studied: chert-rich iron-bearing rocks, altered volcanic rocks, and banded iron formations. Sample AB-11-41, collected from the Abitibi formation, is shown in image A. The large nodules of quartz encased by rims of finer grained quartz are lapilli. The matrix is composed of altered feldspars and clay minerals. Thin section V-19-07, collected from the Vermillion region of Minnesota, is shown in image B. This sample appears to be of volcanic origin, and mineral phases such as altered feldspars, clay minerals, calcite, and chlorite indicate possible alteration by an aqueous source. Image C depicts thin section TEMj-1, collected from the Temagami formation in Ontario, Canada. This sample has a banded appearance consisting of alternating layers of quartz and iron-bearing mineral phases.

### Discussion

The physical appearance and mineral composition of these rocks can be helpful in discerning the process through which the rocks formed. We believe there are two primary methods of deposition for these iron formations: chemical sedimentation and silicification. Chemical sedimentation involves ions concentrating in the water column and being precipitated out. In the samples that display well ordered bands of iron and silica, chemical sedimentation is the likely mechanism of formation (Figure 2, image C). We also believe it is possible that the chert-rich iron-bearing rocks formed through silicification, where the original minerals of the rock are replaced with silica that is circulated through by an aqueous source (Breneman et al., 2020).

Evidence of silicification includes the presence of preserved volcanic features (lapilli) and the microcrystalline quartz that can be found in sample AB-11-32.

The mechanism of formation can give us clues about the depositional environment of the sample. Both silicification and chemical sedimentation can occur in a subaqueous and hydrothermally active environment. It is possible that the method of deposition can also tell us about proximity to high-temperature activity such as volcanism. In a modern spreading center environment, silicification is prevalent in deep water that is farther from the volcanic source and has a lower water temperature. Chemical sedimentation indicates a warmer water temperature because of its closer proximity to the spreading center. If we were to apply this assumption to the Precambrian, then we could say that the samples that present signs of silicification originated farther from a volcanic source than those of chemical sedimentary origin. Silicification also requires significant amounts of concentrated silica in the water column. This suggests the possibility that samples showing signs of silicification are in closer proximity to a VMS deposit, where silica content tends to increase, and would therefore encourage silicification of existing rocks (Lentz & Goodfellow, 1996).

### **Conclusion**

Based on preliminary data, it appears that chemical sedimentation was the predominant depositional process for iron formations in the Temagami region; silicification was prominent in the Abitibi region; and the Vermillion region seems to have both silicification and chemical sedimentation. However, further investigation is necessary to assess the validity of these observations. It would be ideal to collect and analyze a greater number of samples to consider the role of each method of deposition on a larger scale. Geochemical analysis of the silica and oxygen isotope values of these samples would also be helpful to determine the accuracy of these claims (Brenngman et al., 2020).

## References

1. Brengman et al. (2020), Constraining mechanisms of quartz precipitation during silicification and chemical sedimentation in the ~2.7 Ga Abitibi Greenstone Belt, Canada. EarthArXiv.
2. Brengman, L. A., Fedo, C. M. (2018). Development of a mixed seawater-hydrothermal fluid geochemical signature during alteration of volcanic rocks in the Archean (2.7 Ga) Abitibi Greenstone Belt, Canada. *Geochimica et Cosmochimica Acta*. 227, 227-245.
3. Brengman, L. A., Sheik, C. (2018). Soudan geomicrobiology field guide. P. 1-4.  
Miller, J. D., Jirsa, M.A. (2014). A walk in the park—Neoproterozoic geology of Lake Vermillion
4. Corona, J.C., et al. (2015), The experimental incorporation of Fe into talc: a study using X-ray diffraction, Fourier transform infrared spectroscopy, and Mössbauer spectroscopy. *Contrib Mineral Petrol* 170, 29.
5. Ericksson, P.G., et al. (1997). Precambrian clastic sedimentation systems. *Sedimentary Geology* 120, 5-53.
6. Lentz, D.R., & Goodfellow, W.D. (1996). Intense silicification of footwall sedimentary rocks in the stockwork alteration zone beneath the Brunswick No. 12 massive sulfide deposit, Bathurst, New Brunswick. *Canadian Journal of Earth Sciences* 33(2), 284-302. State Park: 60th annual meeting, *Institute on Lake Superior Geology*. Proceedings volume 60, Part 2—Field Trip Guidebook, p. 37-41; p. 45-49; p. 62-69.

# Appendix

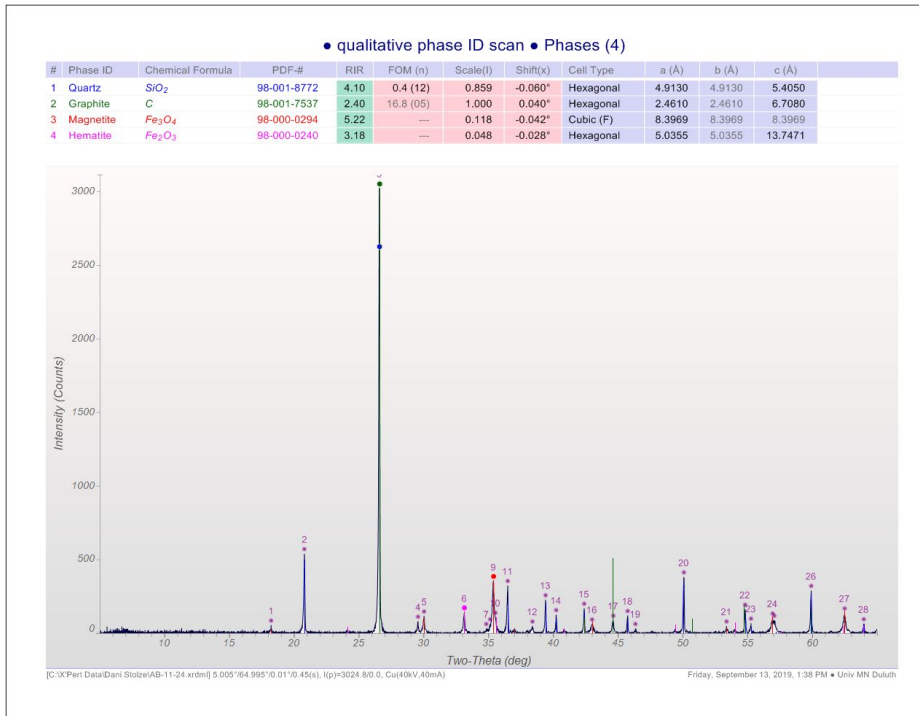


Figure 1. XRD peak matching data for sample AB-11-24. Identified phases include quartz, graphite, magnetite, and hematite. Minnesotaitite, another iron-bearing mineral, may also be present but has not been confirmed by XRD analysis.

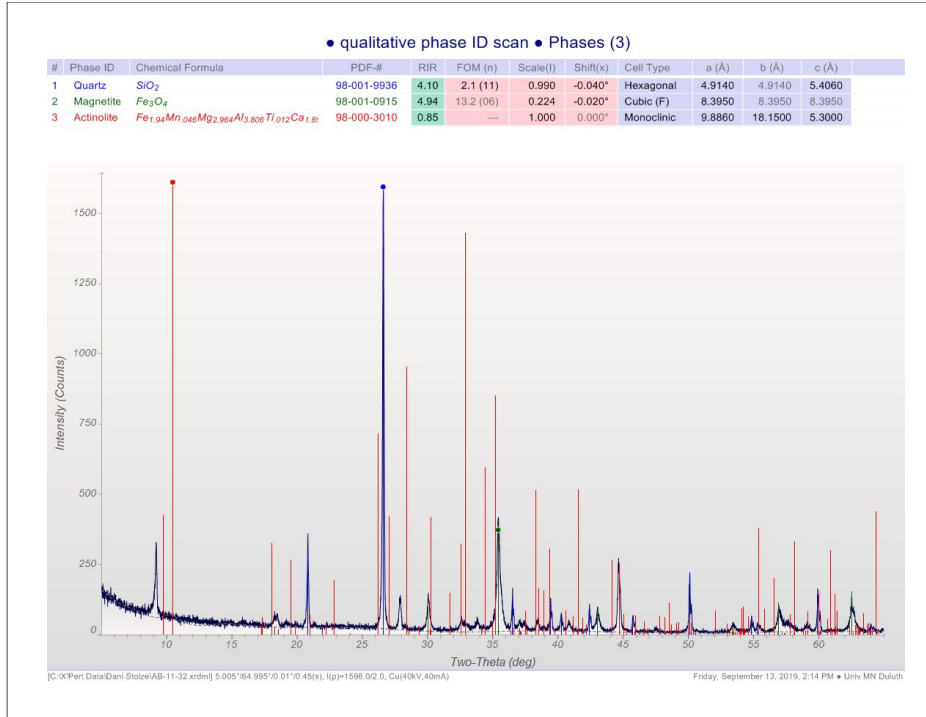


Figure 3. XRD peak matching data for sample AB-11-41. Minerals identified in this sample include quartz, plagioclase (Na rich), graphite, chlorite, prehnite, calcite, and kaolinite. Minnesotaite, another iron-bearing mineral, may also be present but has not been confirmed by XRD analysis.

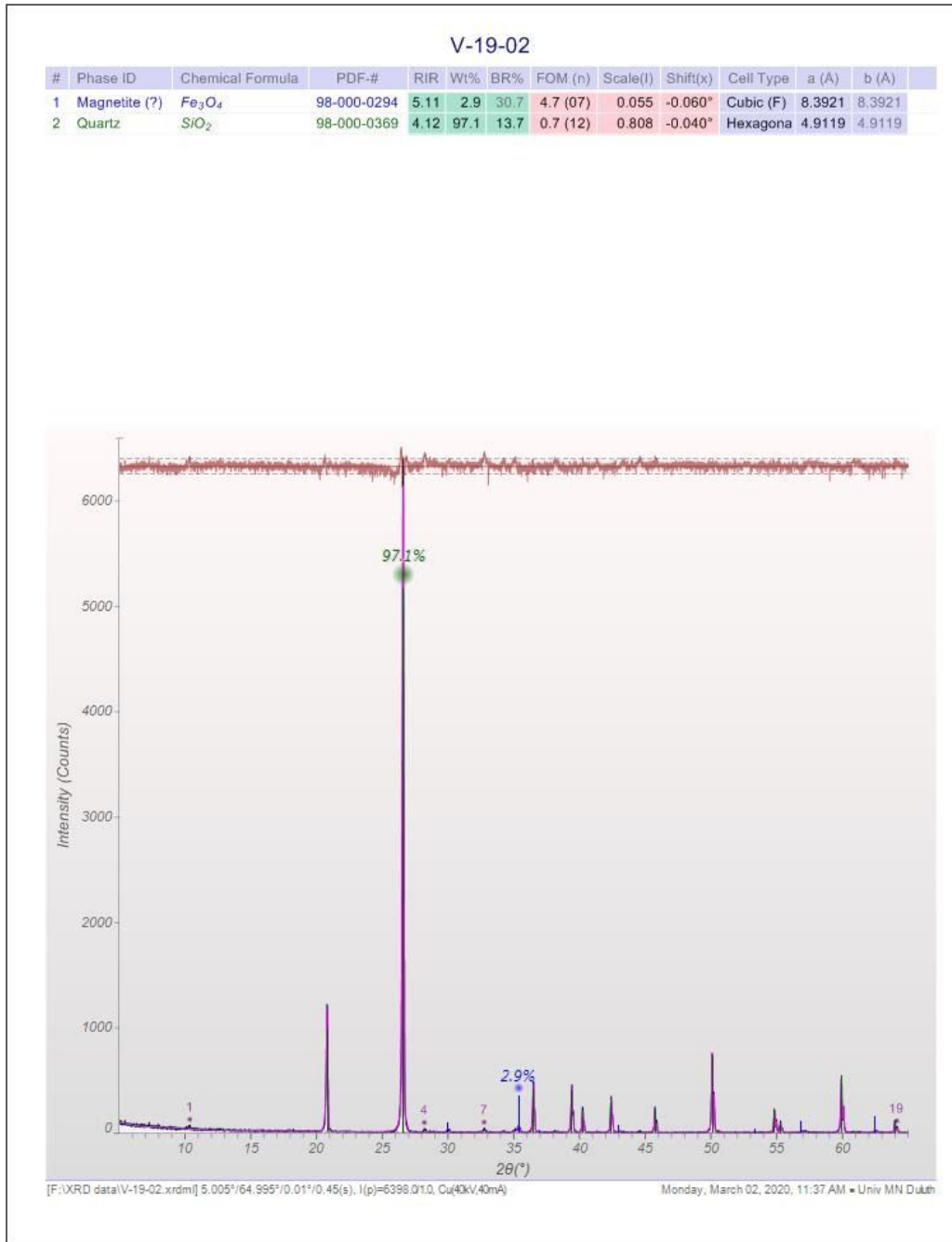


Figure 4. XRD peak matching data for sample V-19-02. Minerals identified in this sample include magnetite and quartz. Minnesotaite, another iron-bearing mineral, may also be present but has not been confirmed by XRD analysis.

V-19-07

#	Phase ID	Chemical Formula	PDF-#	RIR	FOM (n)	Scale(I)	Shift(x)	Cell Type	a (Å)	b (Å)	c (Å)
1	Quartz	SiO <sub>2</sub>	98-000-0369	4.22	0.6 (12)	0.876	-0.080°	Hexagonal	4.9134	4.9134	5.405
2	Albite - low	Na(AlSi <sub>3</sub> O <sub>8</sub> )	98-000-0041	0.65	1.9 (25)	0.193	-0.100°	Triclinic (C-1)	8.1370	12.7850	7.1583
3	Muscovite 2f	KAl <sub>2</sub> [Si <sub>3</sub> Al]O <sub>10</sub> (OH) <sub>2</sub>	98-000-0321	0.40	9.0 (24)	0.014	0.000°	Monoclinic	5.1890	8.9960	10.0960
4	Calcite	CaCO <sub>3</sub>	98-000-0141	2.99	20.3 (06)	0.048	-0.080°	Hexagonal	4.9890	4.9890	17.0620
5	Chlorite - llb	MgFeSiAlOOH	98-000-0159	1.50	---	1.000	0.000°	Triclinic (C-1)	5.3560	9.2070	14.3600

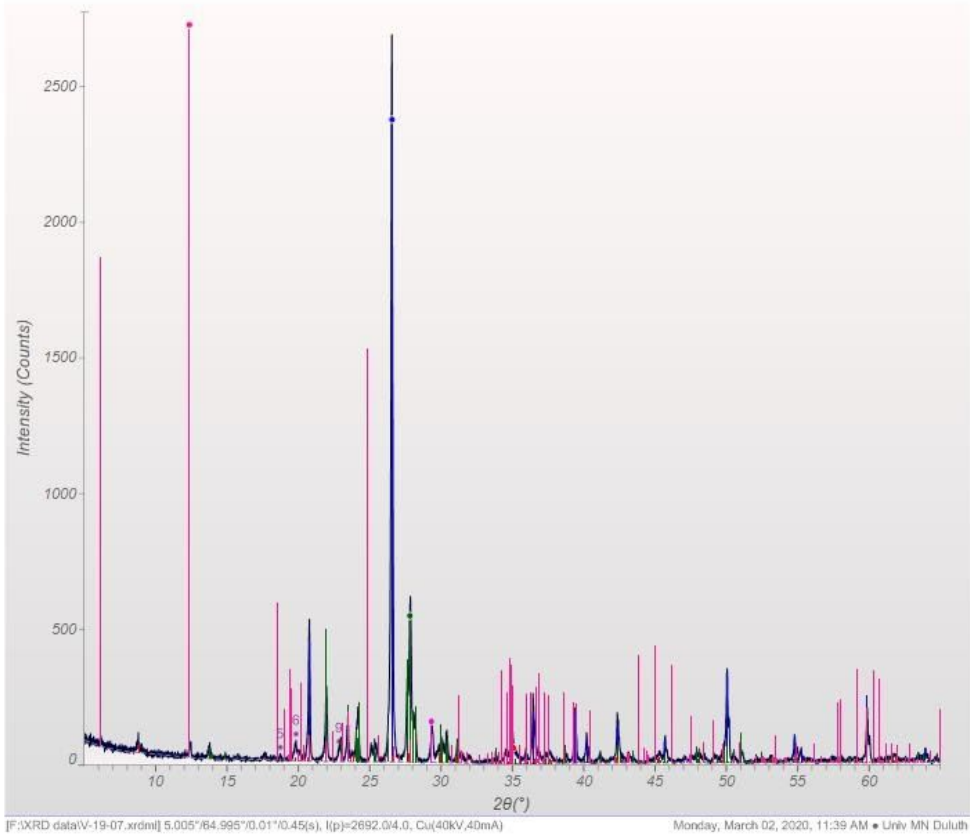


Figure 5. XRD peak matching data for sample V-19-07. Minerals identified in this sample include quartz, plagioclase (albite), muscovite, calcite, and chlorite.